A model-based Direct Power Control for Three-Phase Power Converters

Sergio Vazquez. *Student Member, IEEE*, Juan Antonio Sanchez, Juan Manuel Carrasco, *Member, IEEE*, Jose Ignacio Leon, *Member, IEEE*, Eduardo Galvan, *Member, IEEE*

***Abstract*— Direct Power Control (DPC) technique has been widely used as control strategy for three-phase power rectifiers due to its simplicity and good performance. The DPC uses the instantaneous active and reactive power to control the power converter, the controller design has been proposed as a direct control with a look up table (LUT), and in recent works, as an indirect control with an inner control loop with proportional plus integral controllers for the instantaneous active and reactive power errors. In this paper a model-based DPC for three-phase power converters is designed, obtaining expressions for the input control signal which allow to design an adaptive control law minimizing the errors introduced by the parameters uncertainties as the smoothing inductor value or the grid frequency. Controller design process, stability study of the system and experimental results for a synchronous three-phase power rectifier prototype are presented to validate the proposed controller.**

***Index Terms*— Adaptive control, direct power control, power factor correction, power quality, three-phase power converters.**

I. Introduction

Power rectifiers are well-known power systems for industrial applications as DC-bus supply to three-phase vector-controlled PWM inverters and DC-Loads and for the integration of renewable energy applications. Not controlled three-phase rectifiers have been widely used due to its reliability, robustness and low cost, at the expense of introducing energy losses in the transmission line and harmonic currents into the grid that not fulfil the new standards for the electric grid, IEEE-519 for USA and IEC 61000-3-2 and 61000-3-4 for Europe [1]-[4]. Due to these facts new power converter topologies and their control strategies fulfilling with these standards have been developed and studied in recent years [5]-[18]. Among these topologies, PWM regenerative rectifiers (Fig. 1) have some extra advantages as: bidirectional power flow, almost sinusoidal currents, near unity power factor and regulation of dc-link voltage. Due to these facts the control of these power systems is currently one objective for the researchers. One of the most efficient control strategies for this system is Direct Power Control (DPC). DPC control strategy lies on the instantaneous reactive power theory introduced by Akagi et al. [19] and is based on the evaluation of the active and reactive instantaneous power errors values and the voltage vector position [20] or the Virtual-Flux vector position [21] without any internal control loop for the currents. The basic idea of DPC is to choose the best state of the power switches among the eight possible states in order to maintain the DC-Link voltage constant, and to keep the unity power factor. The vector selection is made through a Look Up Table (LUT), where the input variables are the voltage grid vector position and the instantaneous active and reactive power errors. This controller has the behaviour of a bang-bang controller, so the authors usually include a hysteresis band in order to reduce the controller gain. One drawback of this DPC controller is that it has not a constant switching frequency and in order to overcome this fact Pulse Width Modulation (PWM) and Space Vector Modulation (SVM) with constant switching frequency have been introduced [22]-[27]. However the main drawback of DPC is the high gain of the controller, and as consequence, the values of the input inductors have to be very large to attenuate the current ripple, increasing the cost, size and weight of the system. In order to reduce the input inductors values, LCL filters have been proposed to connect the power converter to the grid [28]-[30]. That solution has the drawback of the filter resonance so it has to be well studied. Besides, recently works have introduced predictive control strategies for the DPC [31]-[32].

Applications based on DPC have demonstrated that it is a simple and efficient control strategy achieving good dynamic performance and near unity power factor. However the smoothing inductances used to connect the power converter to the grid are still too large, increasing the cost, size and weight of the total system and reducing dynamics and operation range of PWM rectifier [33]. A controller design based on the system model can overcome this drawback optimizing the power system behaviour. Furthermore adaptive control strategies can be applied to minimize the errors introduced by the parameters uncertainties as the inductor value or the grid frequency.

Manuscript received April 23, 2007. Accepted for publication November 21, 2007. This work was supported in part by the Andalusian Government under grant TIC-1172.

S. Vazquez, J. A. Sanchez, J. M. Carrasco, J. I. Leon, E. Galvan are with the Department of Electronic Engineering, University of Seville, 41092 Seville, Spain (e-mail: svazquez@gte.esi.us.es).

This paper is organized as follows: Firstly the discrete model for a three-phase two-level rectifier is presented. Secondly, based on the system model the direct power control law is derived, and an adaptive control law and the stability study of the system are presented. In the last section of the paper experimental results are included and analyzed in order to verify the theoretical study that has been presented in the previous sections.

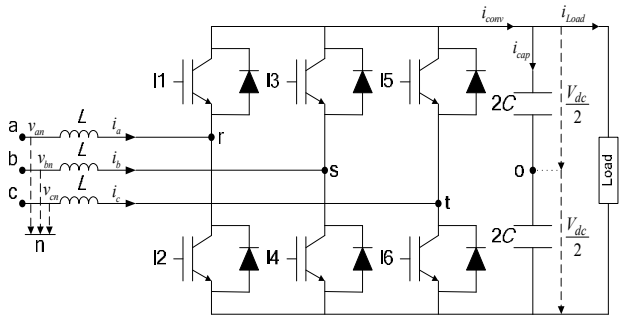

Fig. 1 Three-phase two level power converter.

II. Model of the System

A three-phase two level power converter is depicted in Fig. 1, where the neutral point is denoted by n. The system is connected to the grid through smoothing inductors L, and it is assumed that a pure resistive load R_L is connected at DC-Link capacitor C. The system parameters and variables are described in Table 1.

TABLE 1
SYSTEM VARIABLES AND PARAMETERS

Variable	Description
$v=\{v_a\ v_b\ v_c\}^T$	Phase to neutral input voltage vector
$i=\{i_a\ i_b\ i_c\}^T$	Phase input current vector
$\delta=\{\delta_a\ \delta_b\ \delta_c\}^T$	Control input vector
ω	Grid frequency
L	Smoothing inductor
C	Output capacitor
R_L	Load resistance
V_{dc}	Output capacitor voltage

The equations that describe the input currents dynamics and the output DC voltage dynamic can be derived from the system model. Following the technique presented in [34], the system model can be obtained in the stationary $\alpha\beta$ frame [23].

$$v_{\alpha\beta} = L\cdot\frac{di_{\alpha\beta}}{dt}+\frac{V_{dc}}{2}\delta_{\alpha\beta} \tag{1}$$

$$C\cdot\frac{d}{dt}\left(\frac{V_{dc}^2}{2}\right)=\frac{V_{dc}}{2}\delta_{\alpha\beta}^T i_{\alpha\beta}-\frac{V_{dc}^2}{R_L} \tag{2}$$

$$\delta_{\alpha\beta}=A\delta=\begin{bmatrix}u_\alpha & u_\beta\end{bmatrix}^T \tag{3}$$

$$A=\sqrt{\frac{2}{3}}\cdot\begin{bmatrix}1 & -\frac{1}{2} & -\frac{1}{2}\\ 0 & \frac{\sqrt{3}}{2} & -\frac{\sqrt{3}}{2}\end{bmatrix} \tag{4}$$

Equations (1) and (2) are the discrete model of the power converter in $\alpha\beta$ coordinates, the $\alpha\beta$ variables can be calculated as $\{\cdot\}_{\alpha\beta}=A\{\cdot\}_{abc}$, where the matrix A is defined by (4). In these equations $\delta_{\alpha\beta}$ has been defined as (3) and it is assumed that V_{dc} is always positive.

Fig. 2 shows the eight possible states of the switches in the $\alpha\beta$ frame, and Table 2 summarizes the possible switch positions in $\alpha\beta$ coordinates.

TABLE 2
AVAILABLE SWITCH POSITIONS IN THE CONVERTER DISCRETE MODEL

State	u_α	u_β
U0	0	0
U1	$2\sqrt{\frac{2}{3}}$	0
U2	$\sqrt{\frac{2}{3}}$	$\sqrt{2}$
U3	$-\sqrt{\frac{2}{3}}$	$\sqrt{2}$
U4	$-2\sqrt{\frac{2}{3}}$	0
U5	$-\sqrt{\frac{2}{3}}$	$-\sqrt{2}$
U6	$\sqrt{\frac{2}{3}}$	$-\sqrt{2}$
U7	0	0

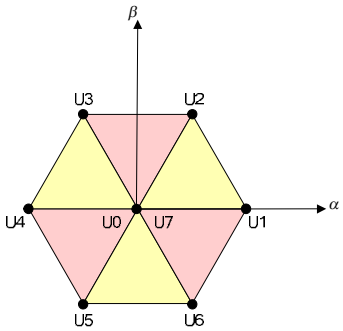

Fig. 2 Switch positions in $\alpha\beta$ frame.

The control objectives for the three-phase power converter are the following:

(i) The instantaneous active power p and the instantaneous reactive power q should track their reference, p^* and q^* respectively, which are calculated in such way that the capacitor output voltage is regulated towards its reference and from the source terminals only instantaneous active power is supplied [19].

$$\begin{aligned} p &\to p^* \\ q &\to q^* \to 0 \end{aligned} \tag{5}$$

Thus, DPC controls indirectly the currents provided by the source through the values of the instantaneous active and reactive power.

(ii) The capacitor output voltage should be regulated towards its reference.

$$V_{dc}\to V_{dc}^* \tag{6}$$

III. CONTROL DESIGN

The proposed controller for the system (1)-(2) is composed of an instantaneous power tracking (inner) loop and a voltage regulation (outer) loop. In what follows is described the design of the two control stages.

A. Instantaneous power tracking loop

The objective of the inner control loop is to guarantee tracking of p and q towards their references. The instantaneous active power reference, p^*, is the output of the outer control loop, and is calculated in order to achieve DC-Link voltage regulation. The instantaneous reactive power reference, q^*, is made zero in order to achieve unity power factor.

In [23], it is shown that in the known parameters case, and assuming that input voltages are balanced and without harmonic content, the instantaneous active power first derivate over the time, $\dot{p}$, and the instantaneous reactive power first derivate over the time, $\dot{q}$, are expressed respectively as

$$L\dot{p} = v_{\alpha\beta}^T \left(\left(1 + \frac{L\omega q}{\left|v_{\alpha\beta}\right|^2} \right) v_{\alpha\beta} - \frac{V_{dc}}{2} \delta_{\alpha\beta} \right) \tag{7}$$

$$L\dot{q} = v_{\alpha\beta}^T J^T \left(-\frac{V_{dc}}{2} \delta_{\alpha\beta} - L\omega p \frac{Jv_{\alpha\beta}}{\left|v_{\alpha\beta}\right|^2} \right) \tag{8}$$

Now the locus of $\delta_{\alpha\beta}$ points where (7) and (8) are made equal to the constants k_1 and k_2 respectively can be calculated.

$$\delta_{\alpha\beta}^{\dot{p}=k_1} = \frac{2}{V_{dc}} \left(L\omega q + \left|v_{\alpha\beta}\right|^2 - k_1 \right) \frac{v_{\alpha\beta}}{\left|v_{\alpha\beta}\right|^2} + c_1 J v_{\alpha\beta} \tag{9}$$

$$\delta_{\alpha\beta}^{\dot{q}=k_2} = -\frac{2}{V_{dc}} \left(L\omega p + k_2 \right) \frac{Jv_{\alpha\beta}}{\left|v_{\alpha\beta}\right|^2} + c_2 v_{\alpha\beta} \tag{10}$$

Equation (9) is the vectorial representation of a straight line in the $\alpha\beta$ frame, where $c_1 J v_{\alpha\beta}$ describes the direction of the line, and c_1 is an arbitrary constant. This line is the set of values of $\delta_{\alpha\beta}$ that makes $\dot{p}$ equal to the constant k_1, and splits the alpha-beta plane in two regions, values of $\delta_{\alpha\beta}$ above (9) make $\dot{p}$ smaller than k_1, while values of $\delta_{\alpha\beta}$ below (9) make $\dot{p}$ larger than k_1.

Equation (10) represents the same idea for the reactive power first time derivate, where $c_2 v_{\alpha\beta}$ describes the direction of the line, and c_2 is an arbitrary constant. $\delta_{\alpha\beta}^{\dot{q}=k_2}$ also splits the alpha-beta plane in two regions, values of $\delta_{\alpha\beta}$ above (10) make $\dot{q}$ larger than k_2, while values of $\delta_{\alpha\beta}$ below (10) make $\dot{q}$ smaller than k_2.

Fig. 3 shows the alpha-beta frame regions where $\dot{p}$ and $\dot{q}$ are enclosed to certain values.

When constants k_1 and k_2 are made equal to zero equations (9) and (10) are respectively transformed in the following expressions [23]

$$\delta_{\alpha\beta}^{\dot{p}=0} = \frac{2}{V_{dc}} \left(L\omega q + \left|v_{\alpha\beta}\right|^2 \right) \frac{v_{\alpha\beta}}{\left|v_{\alpha\beta}\right|^2} + c_1 J v_{\alpha\beta} \tag{11}$$

$$\delta_{\alpha\beta}^{\dot{q}=0} = -\frac{2}{V_{dc}} \left(L\omega p \right) \frac{Jv_{\alpha\beta}}{\left|v_{\alpha\beta}\right|^2} + c_2 v_{\alpha\beta} \tag{12}$$

These two straight lines split the alpha-beta frame in four quadrants as it is shown in Fig. 4. Each zone is characterized by the sign of the instantaneous active and reactive power first derivate over the time, so when the system is working inside one of them the instantaneous active and/or the reactive power can increase or diminish according which work area is. The intersection point between these two straight lines can be calculated as

$$\delta_{\alpha\beta}^{eq} = \frac{2}{V_c} \left(1 + \frac{\omega Lq}{\left|v_{\alpha\beta}\right|^2} \right) v_{\alpha\beta} - \frac{2}{V_c} \left(\frac{\omega Lp}{\left|v_{\alpha\beta}\right|^2} \right) Jv_{\alpha\beta} \tag{13}$$

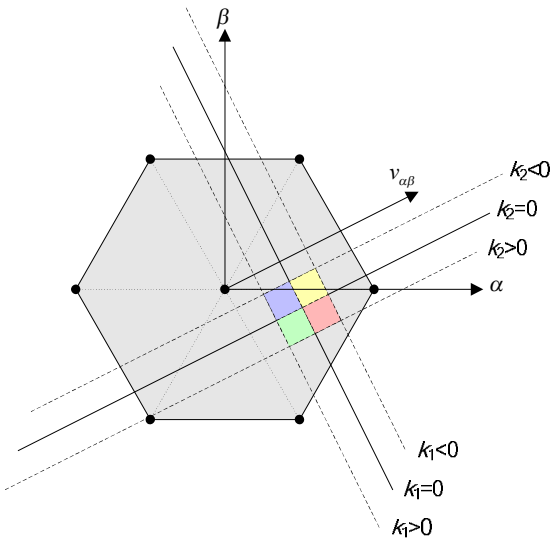

Fig. 3 Boundary limits for the instantaneous active and reactive power first time derivate.

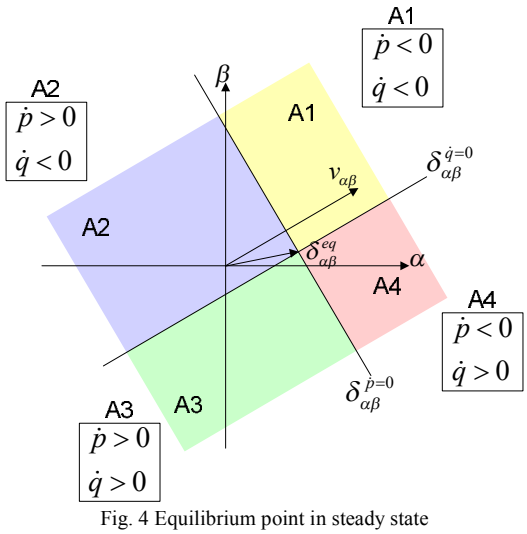

Fig. 4 Equilibrium point in steady state

$\delta_{\alpha\beta}^{eq}$ represents the equilibrium point of the system in steady state due to in this point the instantaneous active and reactive power demanded by the power converter to the power supply do not increase or diminish, and therefore, at this point, the instantaneous active and reactive power demanded by the power converter remain constants.

The following equations define the values of instantaneous active power error, $\tilde{p}$, and instantaneous reactive power error, $\tilde{q}$, respectively.

$$\begin{aligned}\tilde{p} &= p - p^{*} \\ \tilde{q} &= q - q^{*}\end{aligned} \tag{14}$$

The power switches state should be chosen among the discrete possible states inside a selection area defined by the sign of the instantaneous active and reactive power error. Table 3 shows the selection area as a function of the sign of instantaneous power errors.

This basic selection algorithm has the following drawbacks:

1) The possible power switches state is not always unique, i.e. there is more than one possible state for the power switches inside the selection area. Fig. 5 shows a possible situation where in area A2 there are five possible state vectors.
2) The power switches state is not always defined inside the selection area. Fig. 5 shows a possible situation where in area A4 there is not any state vector.

TABLE 3
SELECTION AREA AS FUNTION OF THE INSTANTANEOUS POWER ERRORS

$\tilde{p}$	$\tilde{q}$	Area
>0	>0	A1
>0	<0	A4
<0	>0	A2
<0	<0	A3

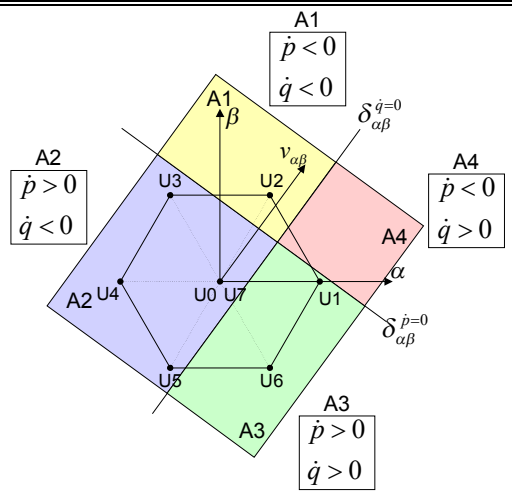

Fig. 5 Power switches states aviable in each selection area.

To overcome these drawbacks in the basic selection algorithm is necessary to define a vector reference that is always in the appropriate selection area, and to generate this reference vector with a modulation technique with a constant switching frequency as PWM or SVM. It is possible to define such a vector reference taking into account the equilibrium point $\delta_{\alpha\beta}^{eq}$ vector value and the involved selection area. The reference vector can be calculated as a composition of the $\delta_{\alpha\beta}^{eq}$ vector, a proportional vector to $v_{\alpha\beta}$ and a proportional vector to $Jv_{\alpha\beta}$. As a function of the selection area, these two last vectors are added or subtracted to the $\delta_{\alpha\beta}^{eq}$ vector to generate the reference vector. In what follows it is presented how the reference vector is composed for each selection area. Besides, a vector diagram including the reference vector and its components is shown in order to demonstrate that the proposed reference vector definition is correct and that the defined reference vector is located inside the appropriate selection area.

For instance, the reference vector in the selection area A1 is defined as follows, where k_1 and k_2 are defined as positive values, ensuring that the reference vector is located inside the selection area A1.

$$\delta_{\alpha\beta} \overset{\Delta}{=} \delta_{\alpha\beta}^{eq} + k_1 \cdot v_{\alpha\beta} + k_2 J v_{\alpha\beta} \tag{15}$$

Fig. 6 shows how reference vector $\delta_{\alpha\beta}$ is composed, and shows that a reference vector defined as (15) is always inside the selection area A1. Due to this fact the proposed reference vector provides the necessary control action to achieve the control objectives, i.e., to reduce the instantaneous active power and to reduce the instantaneous reactive power drawn from the grid.

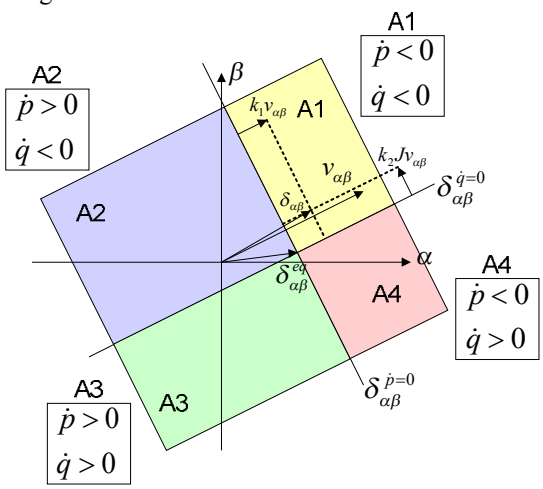

Fig. 6 Reference vector for selection area A1.

Using the same concepts it is possible to define the reference vector $\delta_{\alpha\beta}$ for each area. The proposed algorithm to calculate the reference vector has the following steps:

1) Calculate $\tilde{p}$, and $\tilde{q}$.
2) Set the selection area.
3) Calculate the reference vector

Table 4 summarizes the proposed algorithm to calculate the reference vector.

TABLE 4
REFERENCE VECTOR DEFINITION AS A FUNCTION OF THE SELECTION AREA.

1st Step		2º Step	3º Step
$\tilde{p}$	$\tilde{q}$	Selection Area	Reference Vector
>0	>0	A1	$\delta_{\alpha\beta} = \delta_{\alpha\beta}^{eq} + k_1 \cdot v_{\alpha\beta} + k_2 J v_{\alpha\beta}$
>0	<0	A2	$\delta_{\alpha\beta} = \delta_{\alpha\beta}^{eq} + k_1 \cdot v_{\alpha\beta} - k_2 J v_{\alpha\beta}$
<0	>0	A3	$\delta_{\alpha\beta} = \delta_{\alpha\beta}^{eq} - k_1 \cdot v_{\alpha\beta} + k_2 J v_{\alpha\beta}$
<0	<0	A4	$\delta_{\alpha\beta} = \delta_{\alpha\beta}^{eq} - k_1 \cdot v_{\alpha\beta} - k_2 J v_{\alpha\beta}$

Reference Vector definition in Table 4 can be written in a single equation, reducing the algorithm computational cost, if k_1 and k_2 values are respectively defined as

$$\begin{aligned} k_1 &\triangleq k_p \cdot \tilde{p} \\ k_2 &\triangleq k_q \cdot \tilde{q} \end{aligned} \tag{16}$$

k_p and k_q are defined as a nonzero positive constants, and the proposed reference vector can be calculated independently of the selection area.

$$\delta_{\alpha\beta} \triangleq \delta_{\alpha\beta}^{eq} + k_p \cdot \tilde{p} \cdot v_{\alpha\beta} + k_q \cdot \tilde{q} \cdot Jv_{\alpha\beta} \tag{17}$$

Controller (17) in closed-loop with the system dynamics (7)-(8) provides the following equations

$$\begin{aligned} L\dot{p} &= -\frac{V_{dc}}{2} \cdot \left|v_{\alpha\beta}\right|^2 \cdot k_p \cdot \tilde{p} \\ L\dot{q} &= -\frac{V_{dc}}{2} \cdot \left|v_{\alpha\beta}\right|^2 \cdot k_q \cdot \tilde{q} \end{aligned} \tag{18}$$

Taking into account that in steady state the instantaneous active and reactive reference power are constants then

$$\begin{aligned} L\frac{dp^*}{dt} &= 0 \\ L\frac{dq^*}{dt} &= 0 \end{aligned} \tag{19}$$

$$\begin{aligned} L\dot{\tilde{p}} + \frac{V_{dc}}{2} \cdot \left|v_{\alpha\beta}\right|^2 \cdot k_p \cdot \tilde{p} &= 0 \\ L\dot{\tilde{q}} + \frac{V_{dc}}{2} \cdot \left|v_{\alpha\beta}\right|^2 \cdot k_q \cdot \tilde{q} &= 0 \end{aligned} \tag{20}$$

Equations (20) demonstrate that using the proposed reference vector, the instantaneous active and reactive power errors tend exponentially to zero and the system is stable.

Now an adaptive law with the aim to eliminate the effects of the system parameters uncertainties, the smoothing inductor and the grid frequency value, is derived. In the three-phase power converter the reactance parameter, X, is the product of the smoothing inductor value and the grid frequency.

$$X \triangleq \omega L \tag{21}$$

$$\tilde{X} = \hat{X} - X \tag{22}$$

$$\dot{\tilde{X}} = \dot{\hat{X}} \tag{23}$$

Equation (22) defines the error between the actual value of the reactance and its estimated value $\hat{X}$. Taking into account that parameter X is assumed to be constant or slowly variant, equation (23) defines the error time derivate.

$$\hat{\delta}_{\alpha\beta}^{eq} = \frac{2}{V_{dc}}\left(1 + \frac{\hat{X} \cdot q}{\left|v_{\alpha\beta}\right|^2}\right) v_{\alpha\beta} - \frac{2}{V_{dc}}\left(\frac{\hat{X} \cdot p}{\left|v_{\alpha\beta}\right|^2}\right) Jv_{\alpha\beta} \tag{24}$$

$$\delta_{\alpha\beta} = \hat{\delta}_{\alpha\beta}^{eq} + k_p \cdot \tilde{p} \cdot v_{\alpha\beta} + k_q \cdot \tilde{q} \cdot Jv_{\alpha\beta} \tag{25}$$

Equation (24) is the expression for $\delta_{\alpha\beta}^{eq}$ as a function of the estimated parameter value, and the proposed controller for the three-phase power converter is transformed in (25), introducing the new proposed controller in (7) and (8), the expressions for the power errors dynamics are derived.

$$L\dot{\tilde{p}} = -\frac{V_{dc}}{2} \cdot \left|v_{\alpha\beta}\right|^2 \cdot k_p \cdot \tilde{p} + q \cdot \left(X - \hat{X}\right) \tag{26}$$

$$L\dot{\tilde{q}} = -\frac{V_{dc}}{2} \cdot \left|v_{\alpha\beta}\right|^2 \cdot k_q \cdot \tilde{q} - p \cdot \left(X - \hat{X}\right) \tag{27}$$

To derive an adaptive law to reconstruct parameter $\hat{X}$ a Lyapunov approach is followed. For this purpose a positive-definite function is proposed, where parameter γ is a positive constant that represents the adaptation gain.

$$H = \frac{1}{2}L\tilde{p}^2 + \frac{1}{2}L\tilde{q}^2 + \frac{1}{2 \cdot \gamma}\tilde{X}^2 \tag{28}$$

$$\dot{H} = -\frac{V_{dc}}{2}\left|v_{\alpha\beta}\right|^2 k_p \tilde{p}^2 - \frac{V_{dc}}{2}\left|v_{\alpha\beta}\right|^2 k_q \tilde{q}^2 + \tilde{X}\left(p\tilde{q} - q\tilde{p} + \frac{1}{\gamma}\dot{\tilde{X}}\right) \tag{29}$$

$$\dot{\hat{X}} = \gamma\left(q \cdot \tilde{p} - p \cdot \tilde{q}\right) \tag{30}$$

$$\dot{H} = -\frac{V_{dc}}{2} \cdot \left|v_{\alpha\beta}\right|^2 \cdot k_p \cdot \tilde{p}^2 - \frac{V_{dc}}{2} \cdot \left|v_{\alpha\beta}\right|^2 \cdot k_q \cdot \tilde{q}^2 \tag{31}$$

The time derivate of (28) along the trajectories of (26) and (27) is (29) which is made negative semidefinite by proposing (30) to reconstruct the parameter $\hat{X}$. Finally the time derivate is given by (31).

Following Lasalle´s theorem arguments it can be stated that $\tilde{p} \to 0$ and $\tilde{q} \to 0$ as $t \to \infty$ asymptotically. Moreover, from (30) $\tilde{p} \equiv 0$ and $\tilde{q} \equiv 0$ imply that $\tilde{X}$ is constant. According to (26) and (27) this constant should be zero. This guarantees convergence of the estimated value towards its actual value.

Now taking into account $\tilde{p}$ and $\tilde{q}$ definitions and that q^* is zero with the aim to achieve unity power factor, the parameter $\hat{X}$ can be reconstructed using expression

$$\dot{\hat{X}} = -\gamma \cdot q \cdot p^* \tag{32}$$

B. Voltage regulation loop

The outer control loop is designed to regulate the output capacitor voltage, this voltage should be maintained equal to the DC-Voltage reference value V_{dc}^*.

The voltage capacitor dynamic is defined by (2), and assuming that instantaneous power dynamics are much faster than DC-Voltage dynamic then it is possible to affirm that $p \cong p^*$ and $q \cong 0$, and therefore (2) can be reduced to

$$C \cdot \frac{d}{dt}\left(\frac{V_{dc}^2}{2}\right) = v_{\alpha\beta}^T i_{\alpha\beta} - \frac{V_{dc}^2}{R_L} \tag{33}$$

From Akagi´s power theory the instantaneous active power is defined as $p = v_{\alpha\beta}^T i_{\alpha\beta}$ so the DC-Voltage dynamic equation can be written as

$$C \cdot \frac{d}{dt}\left(\frac{V_{dc}^2}{2}\right) = p - \frac{V_{dc}^2}{R_L} \tag{34}$$

Now, in order to reduce notation, two new variables are defined as follows

$$z \triangleq \frac{V_{dc}^2}{2} \tag{35}$$

$$\tilde{z} \triangleq z^* - z \tag{36}$$

where $\tilde{z}$ represents the error and z^* is the new reference defined as

$$z^* = \frac{\left(V_{dc}^*\right)^2}{2} \tag{37}$$

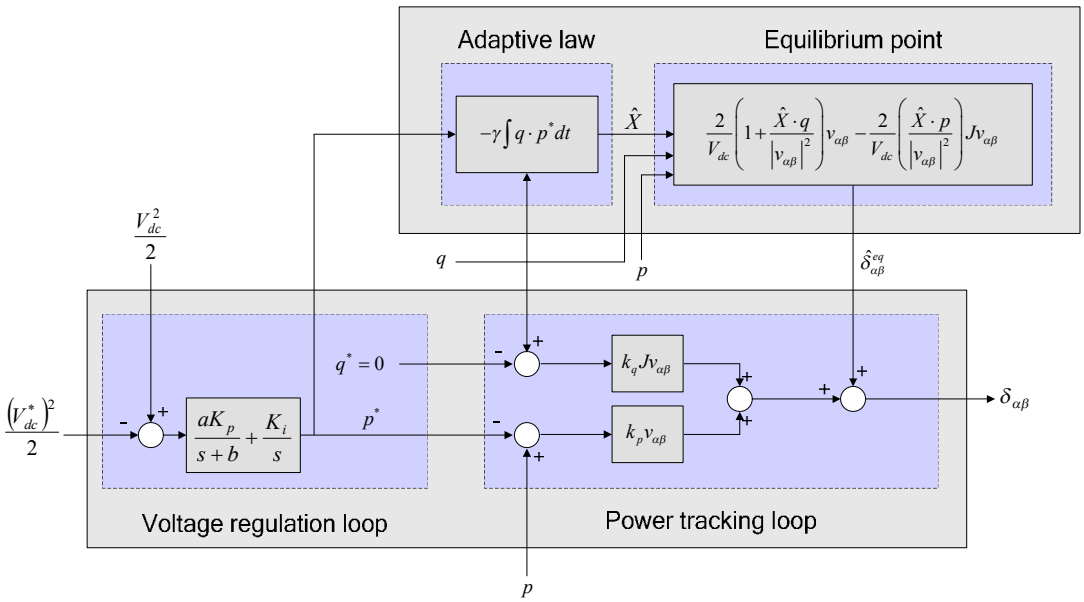

Fig. 7 Block diagram of the proposed DPC controller.

and introducing these news variables in (34)

$$-C\cdot\frac{d}{dt}(\tilde{z})=p+\frac{2\tilde{z}}{R_L}-\frac{\left(V_{dc}^{*}\right)^{2}}{R_L} \tag{38}$$

Notice that (38) is a simple first-order stable system, so a proportional plus integral controller would solve the problem since the perturbation is an unknown constant. Finally the proposed PI controller for the outer control loop is

$$p^{*}=\frac{K_i}{s}\tilde{z}+\frac{K_p}{s+\tau_s}\tilde{z} \tag{39}$$

where K_p, K_i and τ_s are design parameters and $p^{*}$is the reference value for the instantaneous active power. This controller includes a low pass filter in the proportional term to reduce the high frequency noise.

Summarizing, the final expressions for the proposed controller are given by the following equations.

(i) Power tracking loop.

$$\begin{aligned}\dot{\hat{X}}&=-\gamma\cdot q\cdot p^{*}\\ \hat{\delta}_{\alpha\beta}^{eq}&=\frac{2}{V_{dc}}\left(1+\frac{\hat{X}\cdot q}{\left|v_{\alpha\beta}\right|^{2}}\right)v_{\alpha\beta}-\frac{2}{V_{dc}}\left(\frac{\hat{X}\cdot p}{\left|v_{\alpha\beta}\right|^{2}}\right)Jv_{\alpha\beta}\\ \delta_{\alpha\beta}&=\hat{\delta}_{\alpha\beta}^{eq}+k_p\cdot\tilde{p}\cdot v_{\alpha\beta}+k_q\cdot\tilde{q}\cdot Jv_{\alpha\beta}\\ \tilde{p}&=p-p^{*}\\ \tilde{q}&=q-q^{*}\\ q^{*}&=0\end{aligned} \tag{40}$$

(ii) Voltage regulation loop.

$$\begin{aligned}p^{*}&=\frac{K_i}{s}\tilde{z}+\frac{K_p}{s+\tau_s}\tilde{z}\\ \tilde{z}&\overset{\Delta}{=}z^{*}-z\end{aligned} \tag{41}$$

Fig. 7 shows the block diagram of the proposed DPC controller including the adaptive law.

I. Experimental Results

In this section experimental results are shown in order to test the proposed controller using a prototype. For this purpose the three-phase two-level power converter of Fig. 8a has been developed, with a digital implementation of the control algorithm that has been executed in a TMS320VC33 floating point DSP homemade board. The experiment consists of a load step at DC-Link from no-load to full load of 9.375kW. For this purpose capacitor voltage reference has been established to 750V and a 60 Ohm resistive load (Fig. 8b) has been suddenly connected to the DC-Link. To assess the DPC controller with the adaptive law approach, a comparative with the DPC controller without the adaptive law has been carried out. Measurements of DC-Link voltage, phase voltages and currents, harmonic contents of currents, active power, reactive power and power factor, have been taken with a *Fluke 434 power quality analyzer*. Table 5 shows the electrical parameters of the power converter, DC-Link voltage reference, switching and sampling frequencies that have been used in the experimental set up.

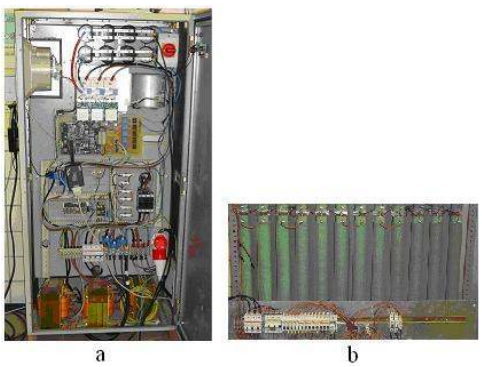

a b

Fig. 8 Laboratory prototype, from left to right: a) Three-phase two level power converter. b) Resistive load of 60 Ω

TABLE 5
ELECTRICAL AND CONTROL PARAMENTERS FOR THE EXPERIMENTAL SYSTEM.

Parameter	Description
Phase-to-neutral Voltage	230 V
Smoothing inductance	0.8 mH
DC-Link capacitor	7050 µF
Resistive load	60Ω
DC-Link Reference Voltage	750 V
Switching frequency	11.2 KHz
Sampling frequency f_m	22.4 kHz

All the constants used in the proposed controller have been adjusted experimentally. This includes, K_p and K_i for the voltage regulation loop, k_p and k_q that provide the necessary damping to the controller, and the adaptation gain γ.

A. *Transient behavior*

Fig. 9 shows DC-Link voltage transient value when load step from zero to full load (9.375kW) is applied to DC-Link. Fig. 9a shows transient response when the proposed non-adaptive DPC controller is applied and Fig. 9b when the proposed adaptive DPC controller is used. It can be noticed that in both cases the transient response is similar. DC-Link voltage only decreases 15 V after the load is connected, and its reference is achieved again only in 0.6s after the load change, so a good voltage regulation is ensured.

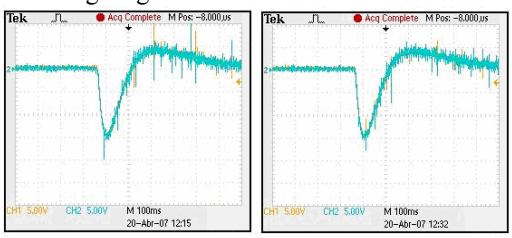

Fig. 9 DC-Link transient voltage during load step from zero to full load. a) for the proposed non-adaptive DPC controller. b) for the proposed adaptive DPC controller

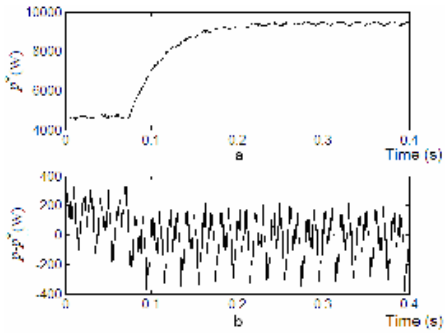

Fig. 10 Instantaneous active power transient responses when load step occurs, from 50 % to full load, for γ = 1e-6. From top to bottom: a) Instantaneous active power reference. b) Instantaneous active power error.

Fig. 10 shows the instantaneous active power transient response when a load step from 50% to full load occurs. From experiments it is observed that the adaptation gain parameter does not have influence in the dynamic and the behavior of the instantaneous active power, for this reason only the transient response when γ = 1e-6 is shown. Fig. 10a shows the instantaneous active power reference value and Fig. 10b the instantaneous active power error when the proposed adaptive DPC controller is used.

Compared with classic DPC, the transient behavior is quite similar, due to when a load step takes place the values of $\tilde{p}$ and $\tilde{q}$ become high and the output of the controller (40) is very close to the vector chosen by the classic DPC. In Fig. 11 a possible case, when p^* and q^* suddenly decrease, is shown.

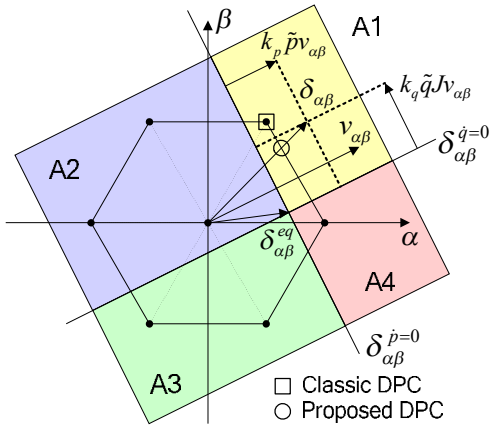

Fig. 11 Comparison between the reference vectors obtained with the Classic DPC (□) and the proposed DPC (○) when the active and reactive instantaneous power references decrease suddenly.

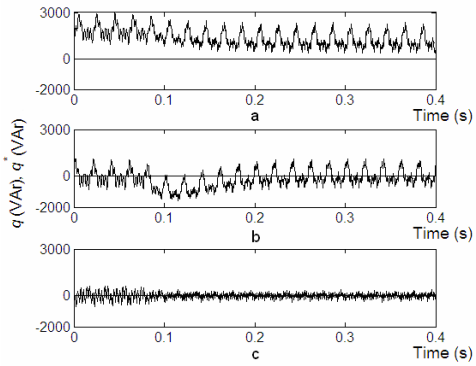

Fig. 12 Instantaneous reactive power transient responses when load step occurs, from 50 % to full load, for different values of γ. From top to bottom: a) γ = 0. b) γ = 1e-8. c) γ = 1e-6.

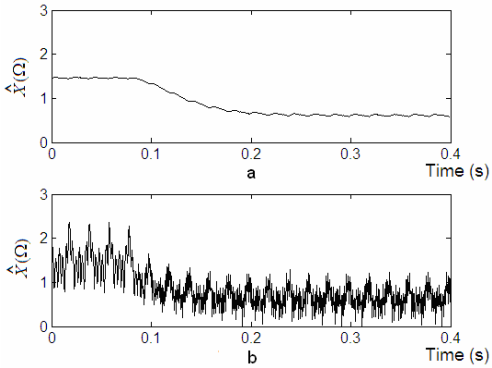

Fig. 13 Estimated value transient responses when load step occurs, from 50 % to full load, for different values of γ. From top to bottom: a) γ = 1e-8. b) γ = 1e-6.

Fig. 12 shows the instantaneous reactive power transient response when a load step from 50% to full load occurs. It can be noticed that the proposed adaptive DPC controller permits

to reduce the reactive power consumption. Fig. 12a shows the instantaneous reactive power when the proposed non-adaptive DPC is used, Fig. 12b and Fig. 12c show instantaneous reactive power when the proposed adaptive DPC is used for different values of the adaptation gain.

Fig. 13 shows the estimated value transient response when a load step from 50% to full load occurs. It can be noticed that $\hat{X}$ ripple increases when the adaptation gain is high. In the experiments it is observed that higher values of γ lead to higher ripples that make system unstable. However, the reactive power consumption is lower as γ increases. Therefore, due to this fact the adaptation gain has to be chosen as high as possible but taking into account the possible system instability.

B. Steady state behavior

Fig. 14(a,b) shows the phase currents achieved with the proposed non-adaptive DPC controller, it can be noticed that low currents distortion is achieved, in fact its total harmonic distortion value (THD) is 3.0% (Fig. 15a). However the current is leading the voltage and the power factor value is 0.99 capacitive as can be seen in Fig. 15b.

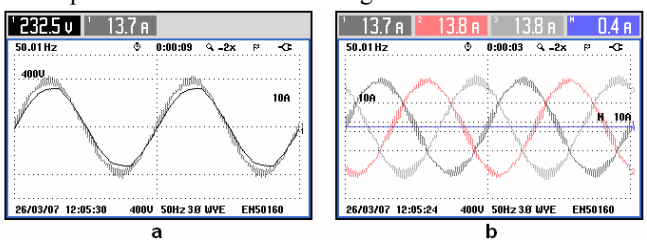

a b

Fig. 14 Phase voltages and currents for the proposed non-adaptive DPC controller. Left to Right: a) Phase c voltage and current. b) a, b and c phase current.

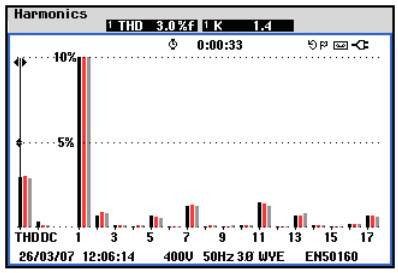

a

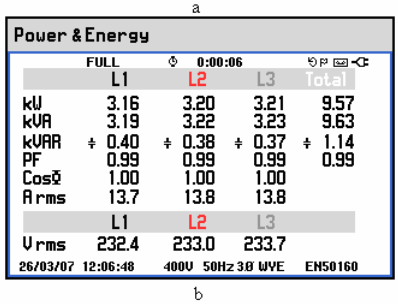

b

Fig. 15 From top to bottom: a) Currents harmonic content for the proposed non-adaptive DPC controller. b) Active and reactive power and power factor for the proposed non-adaptive DPC controller.

Fig. 16(a,b) shows the phase currents delivered by the power converter when the proposed adaptive DPC controller is used. It can be noticed that in spite of the limited smoothing inductance value (0.8mH) the current ripple is small and the current THD is only 3.2% (Fig. 17a). Moreover compared with the phase currents achieved with the non-adaptive DPC controller the harmonic content of currents is of the same order. Besides unity power factor value is achieved as can be seen in Fig. 17b. Due to this fact less reactive power is drawn from the grid, reactive power is drastically reduced in 75% (from 1.14 kVAr in Fig. 15b to 0.3 kVAr in Fig. 17b) and better performance is achieved with the same power converter.

Fig. 18a shows the vector diagram with the proposed non-adaptive DPC controller and Fig. 18b shows the vector diagram with proposed adaptive DPC controller. It can be seen that due to parameters uncertainties when the non-adaptive control law is used voltages and currents are shifted (Fig. 18a). However, when the adaptive solution is adopted, these parameters uncertainties are avoided and voltage and currents are in phase almost perfectly (Fig. 18b), showing the great advantage of using adaptive control techniques.

Fig. 19 shows the instantaneous reactive power value in steady state for different values of γ. As it was presented in Fig. 12 for transient operation, the reactive power consumption decreases when γ increases.

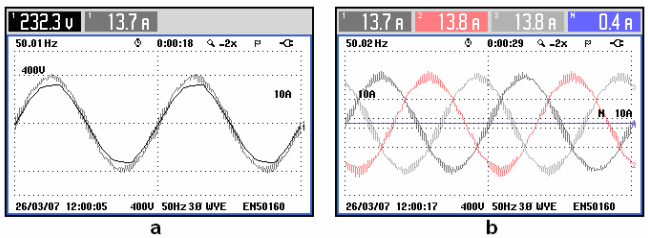

a b

Fig. 16 Phase voltages and currents for the proposed adaptive DPC controller (γ = 1e-6). From top to bottom: a) Phase c voltage and current. b) a, b and c phase current.

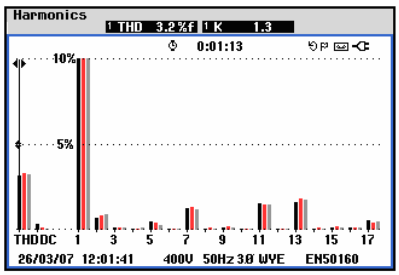

a

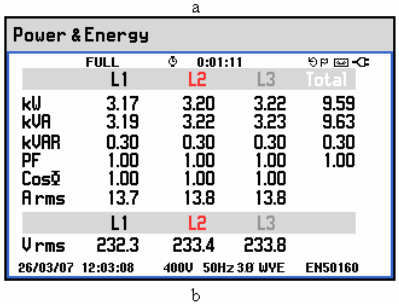

b

Fig. 17 From top to bottom: a) Currents harmonic content for the proposed adaptive DPC controller (γ = 1e-6). b) Active and reactive power and power factor for the proposed adaptive DPC controller (γ = 1e-6).

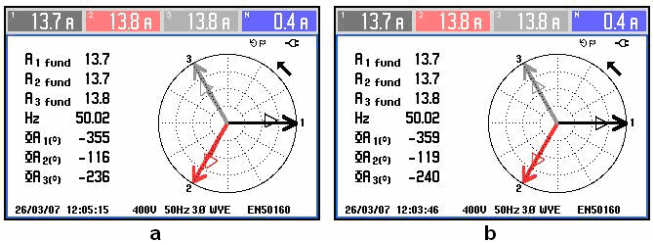

Fig. 18 Vector diagram. From left to right: a) Vector diagram for the proposed non-adaptive DPC controller. b) Vector diagram for the adaptive DPC controller (γ = 1e-6).

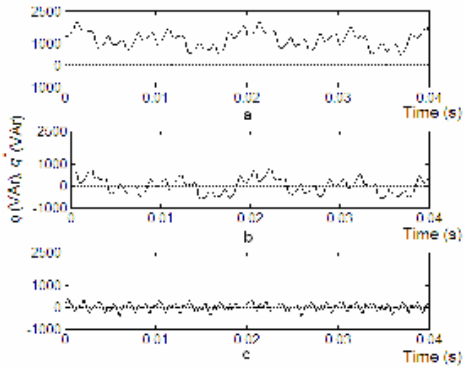

Fig. 19 Instantaneous reactive power steady state values for full load and different values of γ. From top to bottom: a) γ = 0. b) γ = 1e-8. c) γ = 1e-6.

II. Conclusions

DPC strategies are simple and efficient control strategies that can be applied to power systems as power rectifiers allowing the use of low cost microprocessors for their implementation. However, some drawbacks associated to the high grid connection inductance value are present in this type of control techniques. The proposed DPC strategy based on the system model permits to make smooth the high gain of previous DPC techniques and consequently, permits to decrease the smoothing connection inductance value reducing the cost, size and weight of the total system and increasing the operation range of the power converter and improving the dynamics of the system. Experiments with a three-phase two-level laboratory prototype have been carried out to illustrate the good performance of the proposed control technique. Besides, adaptive techniques have been applied to overcome problems associate with system parameters uncertainties, which leads the proposed controller to achieve unity power factor, providing a better performance of the overall system.

References

[1] Recommended Practices and Requirements for Harmonics Control in Electrical Power Systems, IEEE 519, 1993

[2] Limits for Harmonics Current Emissions (Equipment Input Current<16A Per Phase), IEC 1000-3-2 International Standard, 1995

[3] Limits for Harmonic Current Emissions (Equipment Input Current up to and Including 16A Per Phase), IEC 61000-3-2 International Standard, 2000

[4] E.ON Netz Grid Code, Bayreuth; E.ON Netz GmbH. Germany, 1 Aug. 2003

[5] J.R. Rodriguez, J.W. Dixon, J.R. Espinoza, J. Pontt and P. Lezana, "PWM regenerative rectifiers: state of the art", IEEE Transactions on Industrial Electronics, Vol 52, Issue 1, pp. 5 – 22, Feb. 2005

[6] F. Blaabjerg, T. Teodorescu, M. Liserre, and A. V. Timbus, "Overview of control and grid synchronization for distributed power generation systems", IEEE Transactions on Industrial Electronics, vol. 53, Issue. 5, pp. 1398–1409, Oct. 2006

[7] G. Escobar, R. Ortega, H. Sira-Ramirez and H. Ludvigsen, "A Hybrid Passivity Based Controller Design for a Three Phase Voltage Sourced Reversible Boost Type Rectifier", in Proc. 37th IEEE Conference on Decision and Control, Tampa, FL, 1998

[8] S. Fukuda and R. Imamura, "Application of a sinusoidal internal model to current control of three phase utility-interface-converters" IEEE Transactions on Industrial Electronics, vol. 52, Issue 2, pp. 420–426, Apr. 2005

[9] R. Portillo, M.M. Prats, J.I. Leon, J.A. Sanchez, J.M. Carrasco, E. Galvan and L.G. Franquelo, "Modeling Strategy for Back-To-Back Three Level Converters Applied to High Power Wind Turbines" IEEE Transactions on Industrial Electronics, Vol 53, Issue 5, pp 1483 – 1491, Oct. 2006

[10] S. Alepuz, S. Busquets-Monge, J. Bordonau, J. Gago, D. González, and J. Balcells, "Interfacing renewable energy sources to the utility grid using a three-level inverter" IEEE Transactions on Industrial Electronics, Vol. 53, Issue 5, pp. 1504–1511, Oct. 2006

[11] L. Yacoubi, K. Al-Haddad, L.-A. Dessaint and F. Fnaiech, "Linear and Nonlinear Control Techniques for a Three-Phase Three-Level NPC Boost Rectifier", IEEE Transactions on Industrial Electronics, Vol 53, Issue 6, pp. 1908-1918, December 2006

[12] T. Jin and K.M. Smedley, "A Universal Vector Controller for Four-Quadrant Three-Phase Power Converters", IEEE Transactions on Circuits and Systems I: Regular Papers, Vol 54, Issue 2, pp. 377-390, February 2007

[13] Y.A.-R.I. Mohamed and E.F. El-Saadany, "An Improved Deadbeat Current Control Scheme With a Novel Adaptive Self-Tuning Load Model for a Three-Phase PWM Voltage-Source Inverter", IEEE Transactions on Industrial Electronics, Vol 54, Issue 2, pp. 747-759, April 2007

[14] C-T Pan and Y-H. Liao, "Modeling and Coordinate Control of Circulating Currents in Parallel Three-Phase Boost Rectifiers", IEEE Transactions on Industrial Electronics, Vol 54, Issue 2, pp. 825-838, April 2007

[15] C.B. Jacobina, I.S. de Freitas and E.R.C. da Silva, "Reduced-Switch-Count Six-Leg Converters for Three-Phase-to-Three-Phase/Four-Wire Applications", IEEE Transactions on Industrial Electronics, Vol 54, Issue 2, pp. 963-973, April 2007

[16] C. Rech and J.R. Pinheiro, "Hybrid Multilevel Converters: Unified Analysis and Design Considerations", IEEE Transactions on Industrial Electronics, Vol 54, Issue 2, pp. 1092-1104, April 2007

[17] A. Cataliotti, F. Genduso, A. Raciti, and G.R. Galluzzo, "Generalized PWM–VSI Control Algorithm Based on a Universal Duty-Cycle Expression: Theoretical Analysis, Simulation Results, and Experimental Validations", IEEE Transactions on Industrial Electronics, Vol 54, Issue 3, pp. 1569-1580, June 2007

[18] B. Wang, G. Venkataramanan and A. Bendre, "Unity Power Factor Control for Three-Phase Three-Level Rectifiers Without Current Sensors", IEEE Transactions Industry Applications Vol 43, Issue 5, pp. 1341-1348, September/October 2007

[19] H. Akagi, Y. Kanazawa and A. Nabae, "Instantaneous reactive power compensators comprising switching devices without energy storage", IEEE Transactions on Industry Applications Vol. IA-20, pp 625-630, May/June 1984

[20] T. Ohnishi, "Three-phase PWM Converter/Inverter by means of Instantaneous Active and Reactive Power Control", in proc. IEEE-IECON'91, pp 819-824, 1991

[21] M. Malinowski, M. P. Kazmierkowski, S. Hansen, F. Blaabjerg and G. D. Marquez, "Virtual-Flux-Based Direct Power Control of Three-Phase PWM Rectifiers", IEEE Transactions on Industry Applications Vol 37, Issue 4, pp. 1019-1027, July/August 2001

[22] T. Noguchi, H. Tomiki, S. Kondo and I. Takahashi, "Direct Power Control of PWM Converter Without Power-Source Voltage Sensors", IEEE Transactions on Industry Applications Vol 34, Issue 3, pp. 473-479, May/June 1998

[23] G. Escobar, A.M. Stankovic, J.M. Carrasco, E. Galvan and R. Ortega, "Analysis and design of direct power control (DPC) for a three phase synchronous rectifier via output regulation subspaces", IEEE

Transactions on Power Electronics, Vol. 18, Issue 3, pp. 823-830, May 2003
[24] M. Malinowski, M. Jasinski and M. P. Kazmierkowski, "Simple Direct Power Control of Three-Phase PWM Rectifier Using Space-Vector Modulation (DPC-SVM)", IEEE Transactions on Industrial Electronics Vol. 51, Issue. 2, pp 447-454, April 2004
[25] M. Malinowski, G. Marques, M. Cichowlas and M.P. Kazmierkowski, "New direct power control of three-phase PWM boost rectifiers under distorted and imbalanced line voltage conditions" in Proc. IEEE ISIE03, Rio de Janeiro, Brazil, Vol 1, pp 438 – 443, 9-11, June 2003
[26] J. Restrepo, J. Viola, J.M. Aller and A. Bueno "A Simple Switch Selection State for SVM Direct Power Control" in Proc. IEEE ISIE06, Montreal, Canada, Vol 2, pp1112 – 1116, July 2006
[27] S. Vazquez, J. I. Leon, J. A. Sanchez, E. Galvan, J. M. Carrasco, L. G. Franquelo, E. Domínguez and G. Escobar, "Optimized Direct Power Control Strategy using Output Regulation Subspaces and Pulse Width Modulation" in Proc. IEEE IECON06, Paris, France, Vol. 4, pp. 2629-2634, 7-11 Nov. 2006
[28] L. A. Serpa, J. W. Kolar, S. Ponnaluri and P. M. Barbosa, "A Modified Direct Power Control Strategy Allowing the Connection of Three-Phase Inverter to the Grid Through LCL Filters" IEEE Industry Applications Conference 2005, IAS 2005, Vol 1, pp 565-571, October 2005
[29] M. Malinowski, M. P. Kazmierkowski and S. Bernet, "New Simple Active Damping of Resonance in Three-Phase PWM Converter with LCL Filter" IEEE Conference on Industrial Technology, ICIT 2005. pp 861-865, December 2005
[30] L.A. Serpa, S. Ponnaluri, P.M. Barbosa and J.W. Kolar, "A Modified Direct Power Control Strategy Allowing the Connection of Three-Phase Inverters to the Grid Through LCL Filters", IEEE Transactions on Industry Applications, Vol 43, Issue 5, pp. 1388-1400, September/October 2007
[31] S. Aurtenechea, M. A. Rodríguez, E. Oyarbide and J. R. Torrealday, "Predictive direct power control—A new control strategy for dc/ac converters," in Proc. IEEE IECON, Paris, France, pp. 1661–1666, November 2006
[32] S. Aurtenechea, M.A. Rodriguez, E. Oyarbide and J.R. Torrealday, "Predictive Control Strategy for DC/AC Converters Based on Direct Power Control", IEEE Transactions on Industrial Electronics, Vol 54, Issue 3, pp. 1261-1271, June 2007
[33] M. Malinowski, M. P. Kazmierkowski and A. M. Trzynadlowski, "A Comparative Study of Control Techniques for PWM Rectifiers in AC Adjustable Speed Drives", IEEE Transactions on Power Electronics, Vol. 18, Issue. 6, pp 1390-1396, November 2003
[34] V. Blasko and V. Kaura, "A new mathematical model and control of a three-phase AC-DC voltage source converter", IEEE Transactions on Power Electronics, Vol. 12, Issue. 1, pp 116-122, January 1997

Sergio Vazquez (S'04) was born in Seville, Spain, in 1974. He received the B.S. and M.S. degrees in industrial engineering from the University of Seville (US), Seville, Spain, in 2003 and 2006 respectively.
In 2002, he joined the Power Electronics Group, US, working in R+D projects. Currently, he is an Assistant Professor with the Department of Electronic Engineering, US. His research interests include electronic power systems, modeling, modulation and control of power-electronics converters and industrial drives, and power quality in renewable generation plants.

Juan A. Sanchez was born in Morón, Spain, in 1974. He received the B.S. and M.S. degrees in industrial engineering from the University of Seville (US), Seville, Spain, in 2001 and 2004 respectively
He is currently an Assistant Professor with the University of Seville, where he is working on his doctoral thesis on grid power quality. His research interests include power active filters, power control, and wind turbines. He is currently involved in related industrial projects, such as power conditioners for fuel cells and photovoltaic plants.

Juan M. Carrasco (M'97) was born in San Roque, Spain. He received the M.Eng. and Dr. Eng. degrees in industrial engineering from Sevilla University, Sevilla, Spain, in 1989 and 1992, respectively.
He was an Assistant Professor from 1990 to 1995, and is currently an Associate Professor with the Department of Electronic Engineering, Sevilla University. He has been working for several years in the power electronic field where he was involved in industrial application for the design and development of power converters applied to renewable energy technologies. His current research area is distributed power generation and the integration of renewable energy sources.

Jose I. Leon (S'04, M'07) was born in Cádiz, Spain, in 1976. He received the B.S. and M.S. and PhD degrees in telecommunications engineering from the University of Seville (US), Seville, Spain, in 1999, 2001 and 2006 respectively.
In 2002, he joined the Power Electronics Group, US, working in R+D projects. Currently, he is an Associate Professor with the Department of Electronic Engineering, US. His research interests include electronic power systems, modeling, modulation and control of power-electronics converters and industrial drives, and power quality in renewable generation plants.

Eduardo Galvan was born in Aracena (Huelva), Spain, in 1964. He received the M.Sc. degree in electrical engineering and the Ph.D. degree in industrial engineering from the University of Sevilla, Sevilla, Spain, in 1991 and 1994, respectively.
He is an Associate Professor of electronic engineering at the Escuela Superior de Ingenieros, Sevilla. He has been working for several years in the power electronic field where he was involved in the industrial application for the design and development of power converters applied to renewable energy technologies. His research interests include control of power converters (wind turbine applications, active filters, and electric machines).